The development of structure and mechanical properties in poly(ethylene terephthalate) fibres during heat treatment under stress

K.-G. Lee and J. M. Schultz*
Materials Science Program, University of Delaware, Newark, DE 19716, USA
(Received 12 November 1992; revised 4 February 1993)

The development of microstructure during the heat treatment of poly(ethylene terephthalate) fibres has been investigated. Specimens representing different durations (down to a few milliseconds) of isothermal treatment were prepared through interrupted annealing and rapid quenching. Characterization of the structure and properties of such specimens demonstrated that the transformation occurred in two stages. In the first stage, microfibrillar crystals develop. The shrinkage behaviour of the material is set at this stage. In a second stage, the morphology transforms from fibrillar to lamellar. During this process, crystals become increasingly perfect and the crystallinity increases. The stiffness of the fibre increases continuously through these stages.

(Keywords: poly(ethylene terephthalate); fibres; microstructure)

INTRODUCTION

Several investigators[1–4] have measured the kinetics of crystallization from the quiescent melt, and have found that there is a maximum crystallization rate at 180°C, which is independent of poly(ethylene terephthalate) (PET) characteristics and measurement technique. The magnitude of the shortest half-times for transformation are in the range of 16–50 s. Quiescent crystallization from the melt produces a spherulitic crystal aggregate.

There are likewise many reports on the crystallization of oriented PET. In most cases, the starting material is oriented but non-crystalline or poorly crystalline fibre or film. Such specimens are heat treated (annealed) in the solid state to effect crystallization. In such cases the type and extent of constraint imposed on the fibre or film during transformation is an important variable to the kinetics of crystallization and the morphologies in oriented PET.

Dumbleton[5] heat treated drawn PET yarns in their relaxed states. The results pointed towards a folded-chain morphology. Matyi and Crist[6] performed SAXS studies on PET fibres that were drawn and subsequently heat treated with free ends. Disorientation of the scattering entities in fibres annealed at or above 225°C was implied by the change of the four-point SAXS pattern to an arced one. This phenomenon was attributed to the presence of a largely molten structure created during annealing. By comparison with other studies, they speculated that annealing at fixed ends suppressed melting and recrystallization. A model was proposed for PET fibres as a microstructure composed of fibrils separated by non-crystalline material. The crystallization of this material causes the lateral growth of crystals in the fibrils.

Smith and Steward[7] heat treated fibres of varying degree of initial orientation in silicone oil with the fibre length held constant. They observed that the crystallization rate is markedly enhanced by the degree of initial orientation. Crystallization occurred in times of the order of milliseconds in the highly oriented fibres, compared with times of several minutes in unoriented material. Alfonso *et al.*[8] studied the kinetics of crystallization in as-spun PET fibres annealed in an oven with forced circulation of hot air with the temperature near T_g. The orientation of chains in amorphous regions was found to contribute to a remarkable increase in crystallization rate. The effect of the initial orientation on crystallization rate increased with increasing annealing temperature. The dependence of crystallization rate on the initial orientation was, however, found to be lower than that observed by Smith and Steward, probably due to the poor heat transfer rate of air. Althen and Zachmann[9] also used hot air as the heat transfer medium and had findings similar to those of Alfonso. Another observation by these authors was that the final density is independent of the initial orientation.

Fischer and Fakirov[10] and Fakirov *et al.*[11], using SAXS, studied the structure of PET drawn bristles annealed at fixed ends in an oil bath. Their results led to a microstructural model consisting of mosaic blocks with folded chains. In this model, the crystals are highly

* To whom correspondence should be addressed

0032-3861/93/214455-16

defective and there is a gradient of order between crystalline and amorphous regions. The higher the annealing temperature, the more perfect are these crystals. The defects are incorporated in axially oriented domain boundaries within the lamellar crystals.

Gupte *et al.*[12] characterized PET fibres heat treated at constant length in silicone oil. Based on SAXS and WAXS measurements, a two-stage transformation in the fibres was envisioned in the annealing process. In the first stage, defective crystal fibrils form. Internal rearrangements of the structure within the fibrils occur and produce more perfect crystals, separated by more amorphous regions, during the second stage. Substantial disorientation due to relaxation of the tie chains connecting neighbouring crystals was noted in fibres subjected to prolonged annealing with fixed ends. However, Itoyama[13] observes no change in crystal orientation and a marked increase in tensile modulus for oriented PET held under stress upon prolonged heat treatment.

Peszkin *et al.*[14] have studied the kinetics of PET fibres isothermally heat treated at constant load. According to their observations, chain relaxation and crystallization are two competing processes during annealing. At low tension (2.1 MPa), re-coiling of extended chains occurs initially, followed by a slower crystallization. At higher stress and/or temperatures, the crystallization rate increases more rapidly than the rate of re-coiling relaxation and the shrinkage maximum shifts to lower and lower times until the initial shrinkage is no longer observed. At a stress of 5.3 MPa, chain re-coiling still proceeds before crystallization at 100 and 120°C, but the maxima of shrinkage shift to lower times with increasing temperature. Only the crystallization stage is observed at and above 160°C under this stress (5.3 MPa). The crystallization rate increases monotonically with increasing tension or temperature. SAXS measurements show that the average diameter of the fibrils formed in the crystallization is invariant with time during isothermal annealing. However, the WAXS measurements show that the radial angular breadths of crystalline peaks narrow in the heat treatments at the same temperature. The narrowing of the WAXS peaks is thus attributed to the increasing perfection of crystallites.

To a greater or lesser extent, the morphological results on oriented material heat treated under stress cohere with the kinetic/morphological model of Tiller and Schultz[15]. These authors proposed a thermal dendrite model for the crystallization of polymer under high tension. In such a transformation, the heat of fusion generated during crystallization can be dissipated more efficiently by formation of a sharply pointed, rod-like crystal growth front. The incorporation of a large defect concentration into the growing fibrillar crystal can further enhance the crystallization rate because of the lower free-energy difference in crystal and melt.

Many investigators attribute the tensile stress acting on the spinline as the most important single parameter of the spinning process which determines fibre structure and properties. It has frequently been pointed out[15–17] that a high stress during crystallization will provide an additional driving force, owing to a large decrease in the entropy of the non-crystalline material, hence increasing the free-energy difference between this phase and a crystalline state. This driving force can be equivalent to tens or hundreds of degrees of supercooling.

The above brief review demonstrates that considerable effort has been made in structure modelling and/or kinetic study of crystallization in oriented PET. The threadline stress is a very important processing parameter and the crystallization rate is found to be greatly enhanced by this stress. The half-crystallization time is reported[14] to be as short as 20 ms for PET fibres annealed at 200°C and 5.3 MPa. However, threadline stress is seldom the processing parameter chosen by the investigators for their annealing study, probably owing to the difficulties in controlling it without special apparatus. Resolution of structural development in the millisecond range for PET crystallization is also scarce in the literature, probably for the same reason. In a series of studies in the authors' laboratory[12,14,18,19], these problems have been addressed and the physics underlying the crystallization behaviour in PET has been progressively unravelled. A few of the many problems remaining to be addressed are as follows. First, structure development in PET fibres annealed at high temperature (above 200°C) and under high tension during annealing, if known, might provide some useful information on the post-spinning heat-treatment process to increase the tensile modulus of fibres, as well as for the high-speed fibre spinning process. Secondly, a relationship among the processing parameters, the structural morphologies and the corresponding mechanical and other properties, if derived, will help to achieve an optimization of structure and modification of fibre properties.

The present work is undertaken to explore the area that has not been covered by the previous work. Here the threadline tension has been increased to approximately twice the maximum used in the work of Peszkin *et al.*[14]. Heat transfer has been improved, thereby permitting meaningful measurement of activity at small times (an important portion of the kinetic domain).

Peszkin *et al.*[14] studied the heat treatment of PET fibres under low tension. Shrinkage measurements showed that chain re-coiling relaxation was still observable at 100 and 120°C, when the fibres were annealed at the maximum tension (5.3 MPa) used in that work. Therefore, a step towards higher-tension annealing is necessary to realize the crystallization behaviour of PET under high tension. Also, the heat transfer between the fibres and annealing surface in that study is through only one-point contact, which is relatively inefficient. Further, no mechanical properties were measured in that work, although these are very important for an optimization of structure and modification of fibre properties. Mechanical properties can also provide supplementary information on the structural features related to the mechanical performance of materials.

In this work, PET fibres are annealed in hot silicone oil in a good heat transferring environment, as described in the following section. The quenching rate on the annealed fibre is also greatly enhanced by using a quenching solution. Threadline tension can be maintained constant over a wide range. The linear speed of the fibres passing through the annealing device can be increased to the level that the annealing time for the fibres can be lowered to a nominal time interval of 5 ms. Measurements of shrinkage of the annealed fibres at 80°C in water is added to indicate the dimensional stability of the fibres. Systematic mechanical testing has been done to the annealed fibres.

EXPERIMENTAL

Material

PET fibres, supplied by Rhone-Poulenc, were melt spun at 3000 m min^{-1}. Each fibre consists of 22 filaments. Each filament is 18 μm in diameter. The material is non-crystalline, according to its WAXS pattern. The orientation of the molecular chains to the fibre axis is low, as indicated by the birefringence value of 0.035.

Heat-treatment apparatus

The apparatus for annealing fibres, as depicted in *Figure 1*, is composed of five essential parts, which are a take-in device, a tension-control device, a heating device, a quenching device and a take-up device. *Figure 1* is an overview of the heat-treatment apparatus.

The take-in device provides proper feed of fibres into the heat-treatment zone. It consists of two tensioners, a take-in roller, a rubber idle roller, a Teflon® fibre guide and idle rollers. The tensioners were installed between the fibre spool and the take-in roller, to avoid slack movement of the fibre. The take-in roller was driven by a variable-speed motor. The role of the rubber roller was to improve the drivability of the take-in roller over the fibres. The rubber roller was driven by the motion of the take-in roller and its contact with the take-in roller was via pressure from a spring. This pressure could be adjusted by changing the length of the spring. This same set-up was also used in the take-up device. The fibre was wound several times between the take-in roller, Teflon fibre guide and idle roller before it went into the heat-treatment zone.

In the present experiment, the take-in speed was set equal to the take-up speed of the fibres and threadline tension was controlled by passing the fibres through a tension-control device, located between the take-in system and the heating device. The tension-control device is sketched in *Figure 2*. Fibres were passed around a Teflon roller, which sat on a stainless-steel shaft in another Teflon piece of dumbbell shape. This acted as a Teflon shuttle when this whole piece slid in a Plexiglass tube. A specified weight was hung on to the hook on this shuttle by Kevlar® 49 fibres, to exert a constant force on the running fibres. The tension on fibres during the experiments was monitored by static tensiometers.

The heat-treatment device, made of oxidation-free copper, is sketched in *Figure 3*. The fibres passed through a small cavity, with a depth of 4 mm, which was filled

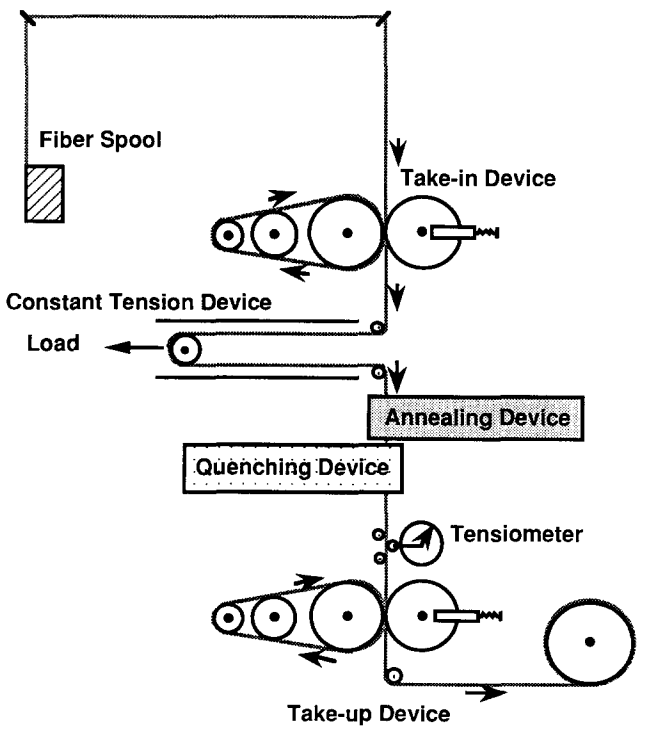

Figure 1 Schematic of the heat-treatment apparatus

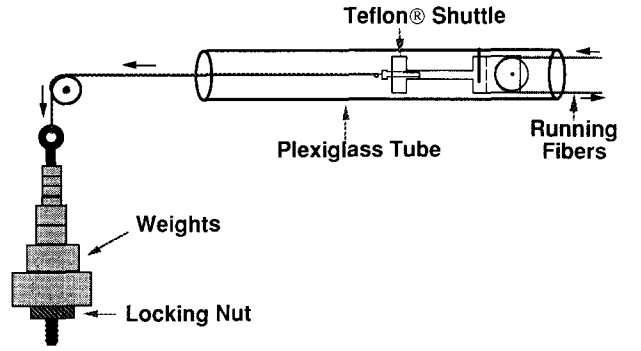

Figure 2 Side view of the tension-control device

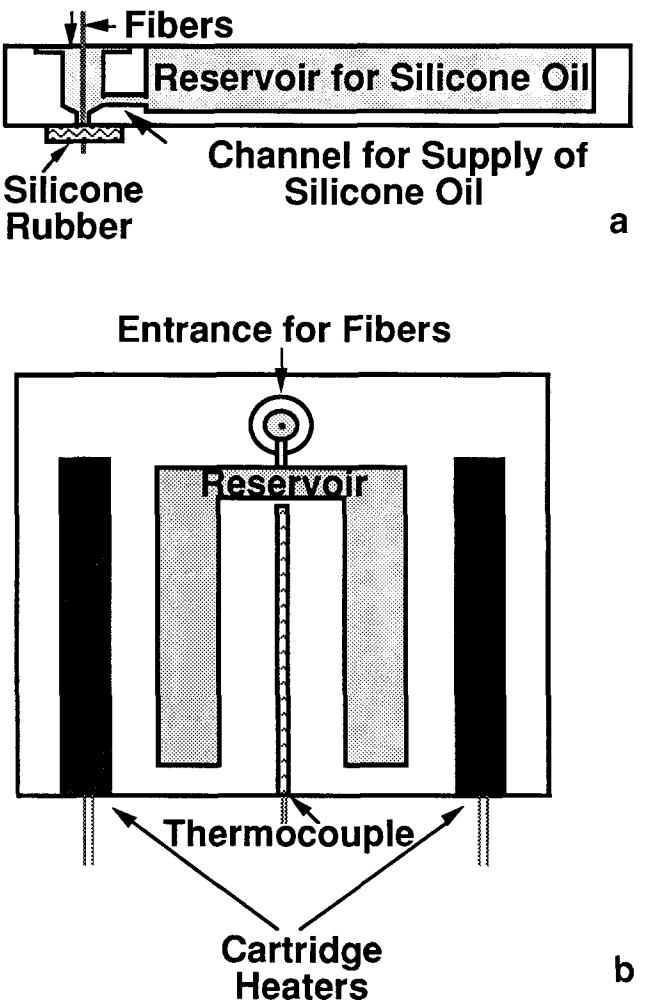

Figure 3 Side view (a) and top view (b) of the device for annealing PET fibres

with silicone oil (Dow Corning 710 Fluid), the heat transfer medium. The level of the silicone oil in this cavity was maintained constant by gravity feed of oil through the channel between this cavity and a reservoir filled with the same oil. The temperature of the silicone oil was kept constant by a temperature controller, a copper/constantan thermocouple and two 15 W cartridge heaters in the device close to the cavity and the reservoir. Below the cavity, a very small hole (0.016 inch (~0.41 mm) in diameter) was drilled through the bottom of the cavity and a piece of silicone rubber was glued to it using a high-temperature epoxy. This silicone rubber was used as a seal to stop silicone oil from flowing out of the cavity and it was porous enough in its internal structure so that it could not exert much resistance to the passage of the fibres and most of the residue silicone oil on the fibres could be scraped off by it when fibres came through. The whole annealing device was mounted on a holder with independent x–y–z positioning.

The structure and property features developed in fibres heat treated under the set conditions were frozen by quenching fibres to a temperature at which mobility of the molecular chains was so low that no further transformation would occur. The quenching device, sketched in *Figure 4*, was situated about 1 mm below the annealing device. The heat-treated fibres passed through liquid trichloroethylene, the quench medium, in an aluminium container, which was in contact with liquid nitrogen. The length of the quenching zone is 1 inch (~25.4 mm). The temperature of this solution was kept at below −40°C. Silicone rubber was also used as the seal in this application. Most of the silicone oil from the heat treatment was washed off in the solvent and some was scraped off when fibres went through the silicone rubber. The temperature of the quenching device was monitored by a temperature controller and an RTD probe.

The heat-treated fibres were collected by a take-up device, which is structurally similar to the take-in device.

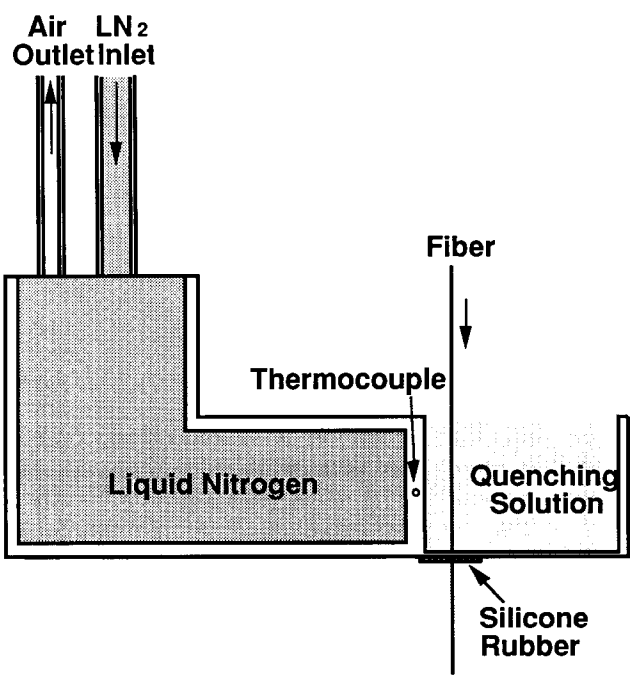

Figure 4 Quenching device for PET fibres

The take-up roller was driven by the motion of a variable-speed motor through a timing belt. The take-in and take-up rollers were connected by a timing belt so that they were synchronized in their start-up and during the heat treatment. The heat-treated fibres were overlaid evenly onto the wind-up spool by a conducting shuttle, moving back and forth transversely.

Annealing conditions

As-spun PET fibres were annealed at 80, 100, 120, 140, 160, 180, 200 and 220°C for a series of nominal time intervals ranging from 5 ms to a few seconds. The threadline tension during heat treatments was 0.083 g/d (1×10^8 dyn cm^{-2}), which was chosen because this stress was reported by George *et al.*[20] and Cheng *et al.*[21] as a critical crystallization stress to induce crystallization in fibre spinning. The stress imposed on the fibres during the annealing is non-uniform over the cross-section. The total stress is the sum of the stress over the skin area and that over the core.

Structure and property measurements

The heat-treated fibres were characterized at room temperature by various methods to follow the kinetics of the development of structure and properties. The procedures for each method are described briefly in the following.

Length-change measurements. Two kinds of length-change measurements were performed: length change due directly to the heat treatment and length change of heat-treated fibres subjected to an additional long-term treatment at 80°C. In both cases, the fibres were first marked at periodic distances before heat treatment, using a water-resistant marker pen. For the first type of measurement, the distance between these marks was measured again after heat treatment and the length change was calculated. In the second type of measurement, the heat-treated fibres were again marked periodically and then put into water at 80°C for 30 s. The distances were then remeasured after the fibres were taken out and blotted dry. This method proved to be a sensitive means of detecting the early stages of crystallization[7,22,23].

The two types of measurement produce rather different information regarding the structure and behaviour of the fibre. During heat treatment well above T_g, threadline stress not only can suppress relaxation of chains, but also can induce crystallization. Whether fibres shrink or elongate in the annealing process is dependent on the threadline stress, as well as the annealing temperature[14]. This measurement enables one to see the effect of threadline force on the crystallization behaviour in PET fibres during annealing.

In the other type of shrinkage measurement, the change in length is measured after an 80°C treatment. This method is based on Wilson's discovery[24] that the 80°C shrinkage of fibres is not caused by chain folding during crystallization as proposed by Dismore *et al.*[25], Statton *et al.*[26] and Dumbleton[27,28], but rather by a disorientation process in the non-crystalline regions. Ikeda[22], following the lead of Smith *et al.*[7] and Adams[23], found this method to be a sensitive means for detecting the early stages of crystallization in PET yarn, while

density, d.s.c. and WAXS methods failed to do so. The reasoning used in interpreting the shrinkage data is as follows: When molecular chains in the amorphous regions are exposed to a temperature just above the glass transition temperature, they relax (re-coil). The extent to which the chains are able to re-coil depends on the magnitude of the restriction exerted on them by either the crystalline phase or the oriented mesophase in the fibres. Therefore, the loss in shrinkage of fibres could be considered an indication of the degree of crystallinity. A temperature of 80°C was chosen because it is above the glass transition temperature for PET and the chains in the amorphous regions have gained enough mobility to relax, while no crystallization at this temperature would be expected in PET fibres when under no constraint at this temperature.

Wide-angle X-ray scattering (WAXS). WAXS studies in the present work are restricted to qualitative observations from flat-film diffraction patterns. WAXS patterns were recorded on film by a pinhole Statton camera with a beam collimator diameter of 0.025 inch (~0.65 mm). Air scattering was avoided by the vacuum environment offered by this camera. Cu K_α radiation was used. The specimen-to-film distance was 5 cm. Fibres were mounted on special sample holders, designed to provide parallel mutual alignment of the fibres.

Small-angle X-ray scattering (SAXS). The SAXS data in this work were collected at the Oak Ridge National Laboratory (ORNL). The SAXS camera at ORNL[29] consists of a graphite-monochromatized Cu K_α rotating-anode X-ray source, a 5 m long evacuated pinhole collimator, a sample chamber, an evacuated scattered beampath section and a two-dimensional position-sensitive detector. A sample-to-detector distance of 5 m was used. The beam size was 1 mm by 1 mm. The fibres were mounted on sample holders with V-shaped grooves to align the fibres parallel to each other. Data were corrected for absorption of the scattered intensity by the sample. The collecting time for each measurement was 30 min.

Density measurements. The densities of the heat-treated fibres were measured using a density gradient column[30], using carbon tetrachloride (density = 1.594 g cm^{-3}) and heptane (density = 0.68 g cm^{-3}).

Mechanical testing. Mechanical properties of the heat-treated fibres were measured by an Instron 1122 tensile testing machine. The data were collected by a Vax computer. The tensile modulus was measured as the slope of the stress–strain curve, using a 10% min^{-1} strain rate and a 500 g load cell. Instron pneumatic action grips were used for clamping the filaments. No slippage of filaments in the grips has been detected during testing by this method. Ten filaments were tested to determine the average mechanical properties for each heat-treatment condition.

The linear densities of the filaments were determined by a vibroscope method. Samples were conditioned in the mechanical testing laboratory at a constant level of 65% relative humidity and 70°F (~21°C) for a minimum of 24 h[31]. Filaments of a specified length were pulled very carefully from each fibre bundle to avoid stretching or damaging the filaments. The linear density (denier) could be computed from the tension, vibrating length and frequency, using:

$$\text{denier} = \frac{2.205 \times 10^8 \times T}{L^2 \times f^2} \quad (1)$$

where T = tension load (g), L = distance between pins (4.10 cm) and f = fundamental resonant frequency.

RESULTS AND DISCUSSION

Characterization

Each of the annealed fibres was characterized at room temperature after annealing. The characterization methods used are shrinkage measurement, density measurement, wide-angle X-ray scattering, small-angle X-ray scattering and mechanical testing.

Density. Density measurement has been widely used in the textile industry as an indication of the extent of crystallization in fibres. Strictly speaking, the apparent mass crystallinity index derived from this measurement based on a two-phase model cannot be treated as the absolute value for crystallinity of fibres. The reason is that there is a multiplicity of orientation states in amorphous regions. A new phase, termed the oriented mesophase, has been inferred by several investigators[18,32–34]. This phase is amorphous as shown by WAXS and has a high orientation. The mesophase likely acts as the precursor of the oriented crystalline phase[34]. Also, the crystalline regions can exist in different states, depending on how perfect these crystals are[11]. The simplistic two-phase model assumes that there are only two states in the material, namely crystalline and amorphous, and each has its absolute density. Nevertheless, density is still a good indication of the relative extent of crystallization.

Figure 5 shows the density evolution of fibres annealed at different temperatures. There is an incubation period for each annealing temperature. The lower the annealing temperature, the longer is the incubation period and the lower is the asymptotic density. The period between when the density begins to increase and when density reaches its asymptotic value is longer the higher the annealing temperature. The asymptotic density increases with treatment temperature, as shown in *Figure 6*. This suggests that the higher mobility of chains at higher

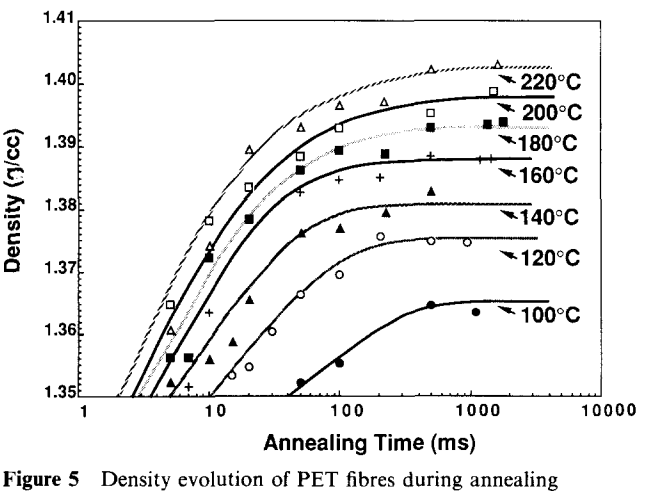

Figure 5 Density evolution of PET fibres during annealing

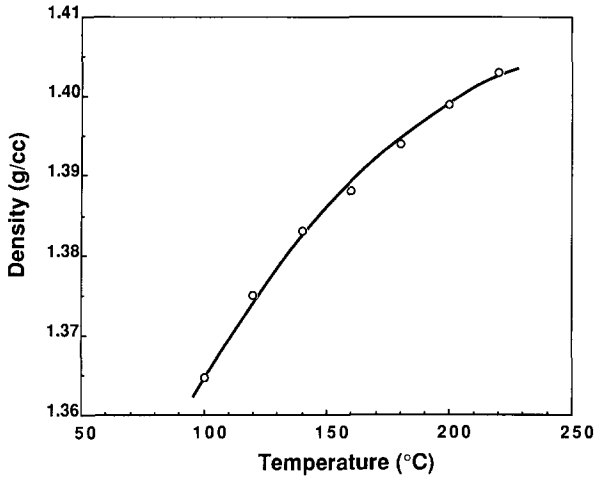

Figure 6 Asymptotic densities of annealed PET fibres *versus* annealing temperature

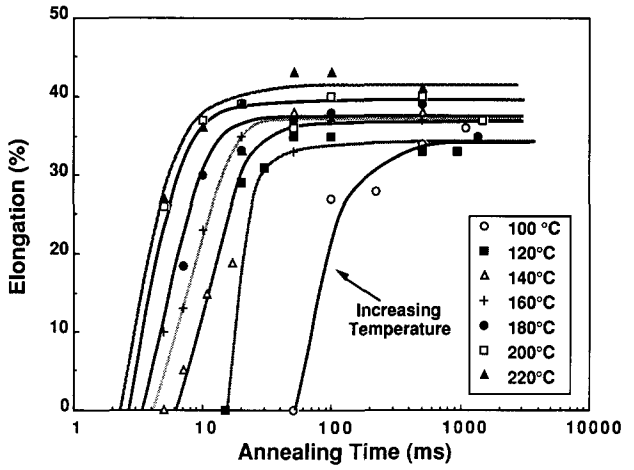

Figure 7 Elongation of PET fibres annealed at different temperatures and time intervals

temperatures enables the crystal to reach a more stable state.

Length change during heat treatment. *Figure 7* shows the change in length due to heat treatment at 0.083 g/d (1×10^8 dyn cm^{-2}). At this stress level, no shrinkage due to the annealing has been observed at any annealing time interval and temperature. Instead, fibres elongated as annealing proceeded, which indicates that the threadline stress (1×10^8 dyn cm^{-2}) is above the re-coiling force of the molecular chains in the fibres at each annealing condition.

According to Peszkin *et al.*[14], chain relaxation and crystallization are two competing processes in the early stage of transformation when PET fibres are subjected to heat and tension. Higher temperature and threadline stress favour crystallization and can suppress relaxation completely. The stress used in this work is 1.89 times higher than the highest stress used in the work of Peszkin *et al.*[14]. The crystallization rate is, therefore, enhanced markedly by the threadline stress, and chain relaxation, as a result, is entirely suppressed in the present annealing experiments. This enhancement in crystallization rate can be best demonstrated for fibres that were annealed at 100°C. In this case the crystalline phase began to emerge at 100 ms, while no crystallization at this temperature had been observed at any time interval (measured up to 1000 ms) at the lower tension levels.

At 100°C, the elongation did not start until some time after 50 ms. Below 50 ms, there is no shrinkage or elongation observed. For 120 and 140°C, the incubation periods before elongation started are some 15 and 5 ms, respectively. When the annealing temperature is over 140°C, the incubation period falls below 5 ms, which is beyond the minimum annealing time interval achievable in these annealing experiments. The time interval between the start of elongation and when it reached its asymptotic value decreases with increasing annealing temperature, as seen in *Figure 7*. For example, the period for 100°C is 500 ms, while only approximately 10 ms was needed for 200°C.

In a later section, a comparison will be made between the characteristic time for the start of elongation, the shrinkage at 80°C, the emergence of the crystalline phase (measured by WAXS) and the emergence of the interference maximum in SAXS.

Shrinkage at 80°C. In *Figure 8* is plotted the variation of the 80°C shrinkage of as-spun fibres that have been cold drawn to different extents at room temperature. As can be seen, shrinkage can be suppressed markedly even by cold drawing when the deformation is over 60%, which is the natural draw ratio. In this regime (over 60%) shrinkage decreases with increasing deformation. The suppressing mechanism on shrinkage behaviour, in this case, is likely due to the highly oriented mesophase, which forms when the tensile stress orients molecules in the amorphous region. When molecular chains become highly oriented, the intramolecular interaction is strong enough to lock these chains in place and contribute to a decrease of chain mobility in the amorphous area. The point of no return for shrinkage at 60% deformation seems to suggest that a critical mesophase density for restricting chain movements is reached at this deformation. Below 60% deformation, the shrinkage increases with increasing deformation. This observation indicates that some of the deformation is reversible when the molecular chains gain enough mobility. The shrinkage value of 52% for the as-spun fibre is believed to be set by the processing history of the fibre.

The 80°C shrinkage evolution curves for the annealed fibres are of sigmoidal shape, as shown in *Figure 9*. The incubation period for the shrinkage decrease increases

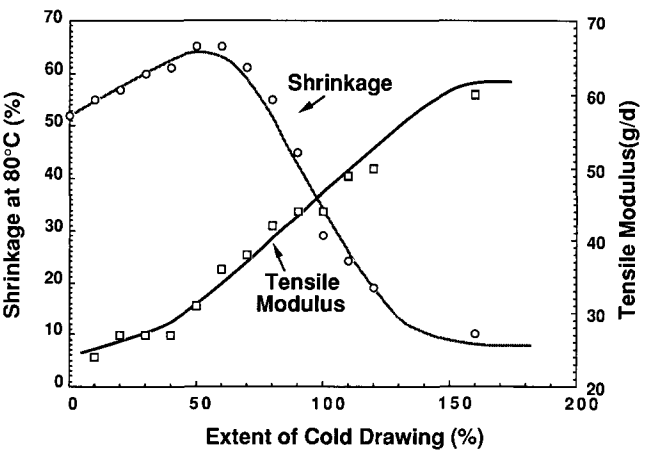

Figure 8 Shrinkage at 80°C and tensile modulus of PET fibres drawn to different extensions

with decreasing temperature. The shrinkage decreases to near zero before the density reaches its asymptote (see *Figure 5* and, later, *Figure 22*). Thus it appears that 80°C shrinkage represents the extent of crystallization only in the early stage of transformation.

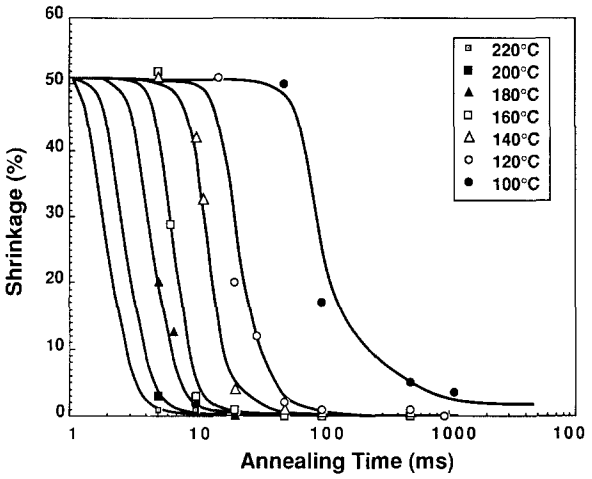

Figure 9 Shrinkage at 80°C for annealed PET fibres

Wide-angle X-ray scattering (WAXS). *Figure 10* shows WAXS pinhole patterns of PET fibres annealed at different time intervals and different temperatures. A comparison of the patterns of the annealed fibres and the predicted pattern for *c*-axial orientation indicates that the *c* axis of the crystallites aligns very closely — if not parallel — to the fibre axis. The orientation of the crystallites to the fibre axis is controlled by the orientation of the taut tie chains bridging these crystallites in amorphous regions. Therefore, a high orientation of the crystallites to the fibre axis cannot be achieved without a high orientation of molecular chains that connect crystallites. If the taut tie chains are poorly aligned to the fibre axis, the crystallites they bridge will be tilted and cause the (1 0 0) reflection peak to move away from the equator. The tilting of crystallites in PET fibres was observed by Gupte *et al.*[12] and Peszkin *et al.*[14], when PET fibres were annealed with fixed ends or under low tension. The orientation of the taut tie chains is believed[35] to have a large influence on the mechanical properties of the material. The more oriented the tie chains to the fibre axis, the higher is the tensile modulus.

One common trend observed in the WAXS patterns of the annealed fibres is that the higher the annealing

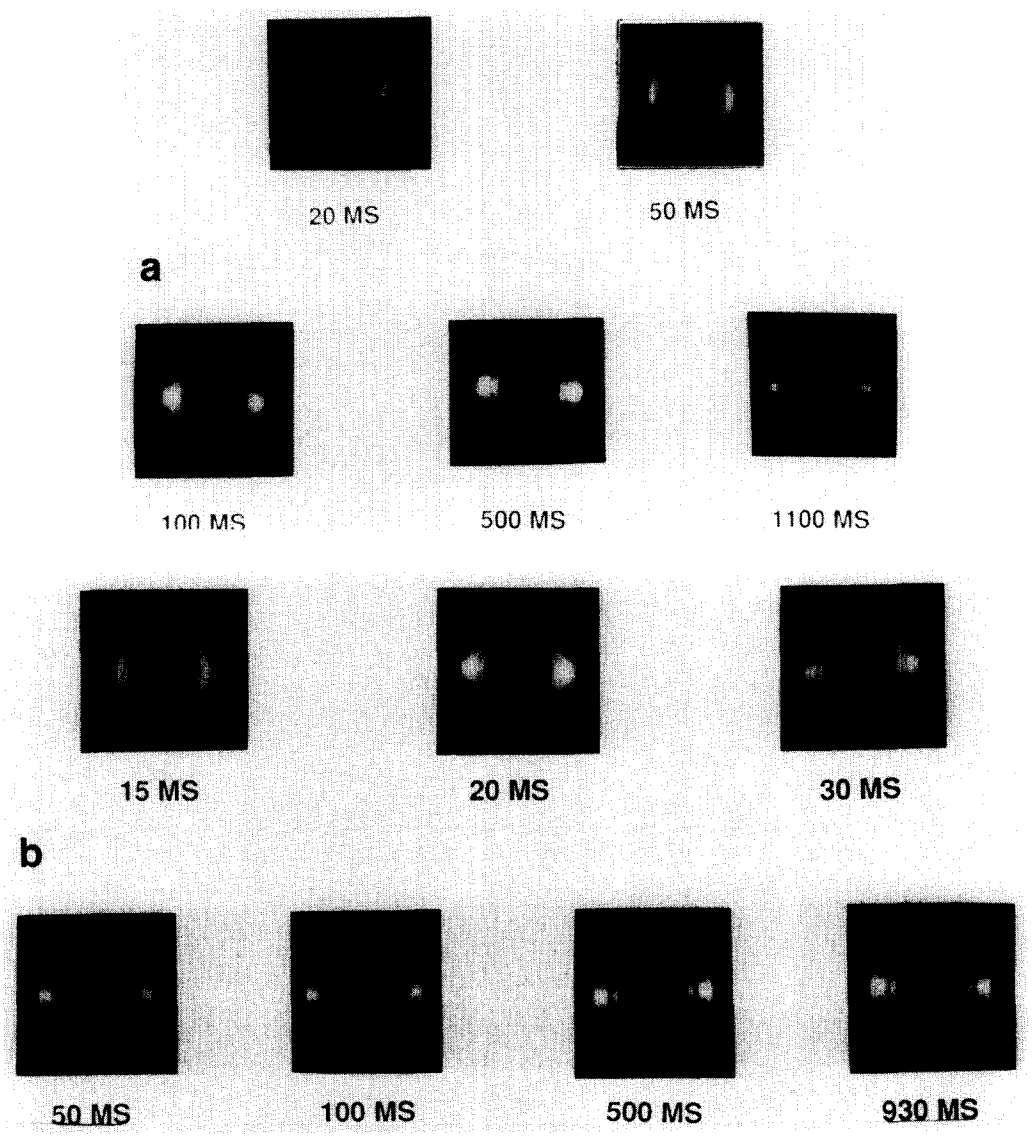

Figure 10 WAXS pinhole patterns of PET fibres heat treated at 0.083 g/d and (a) 100, (b) 120, (c) 140, (d) 160, (e) 180, (f) 200 and (g) 220°C, for times indicated. The fibre axis is vertical

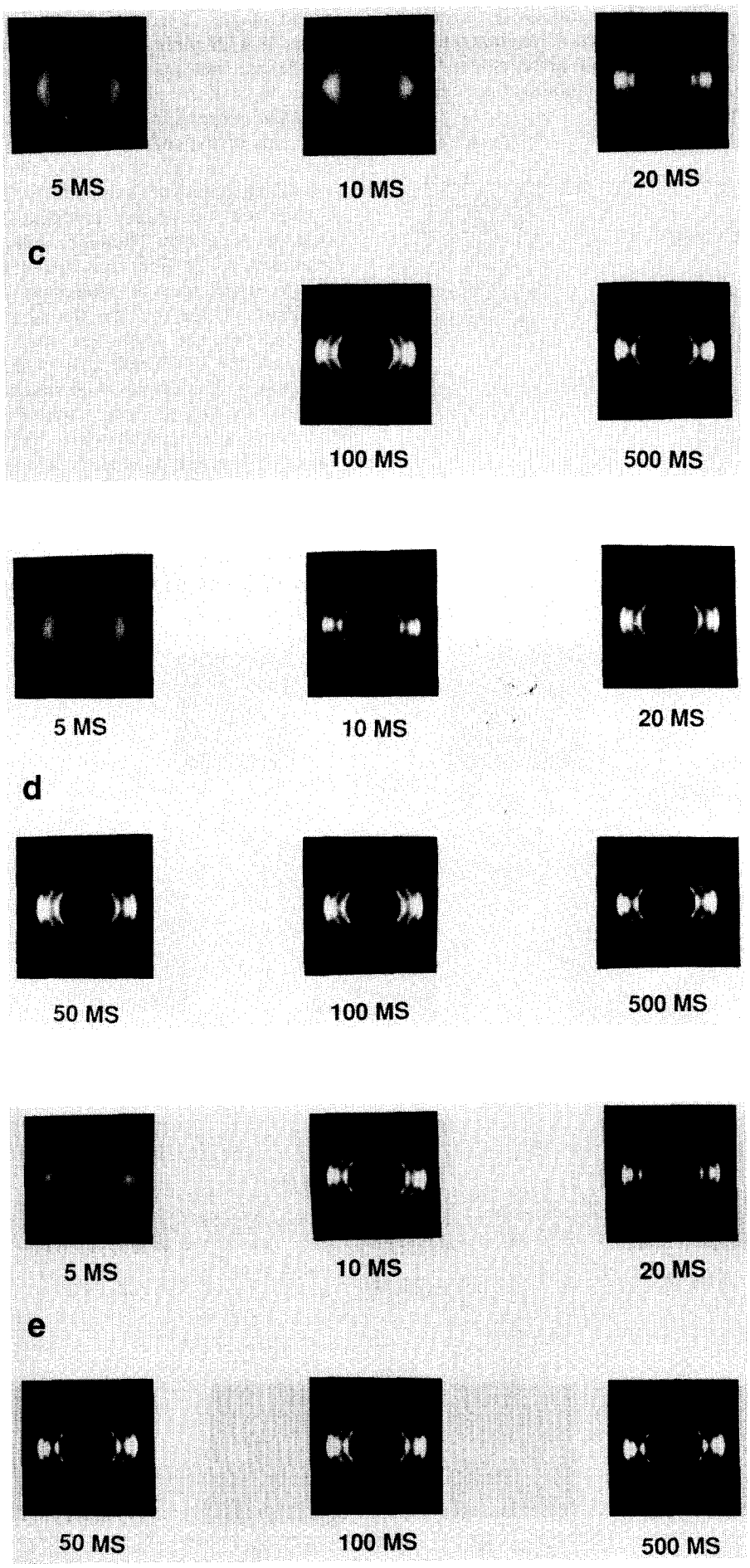

Figure 10 *continued*

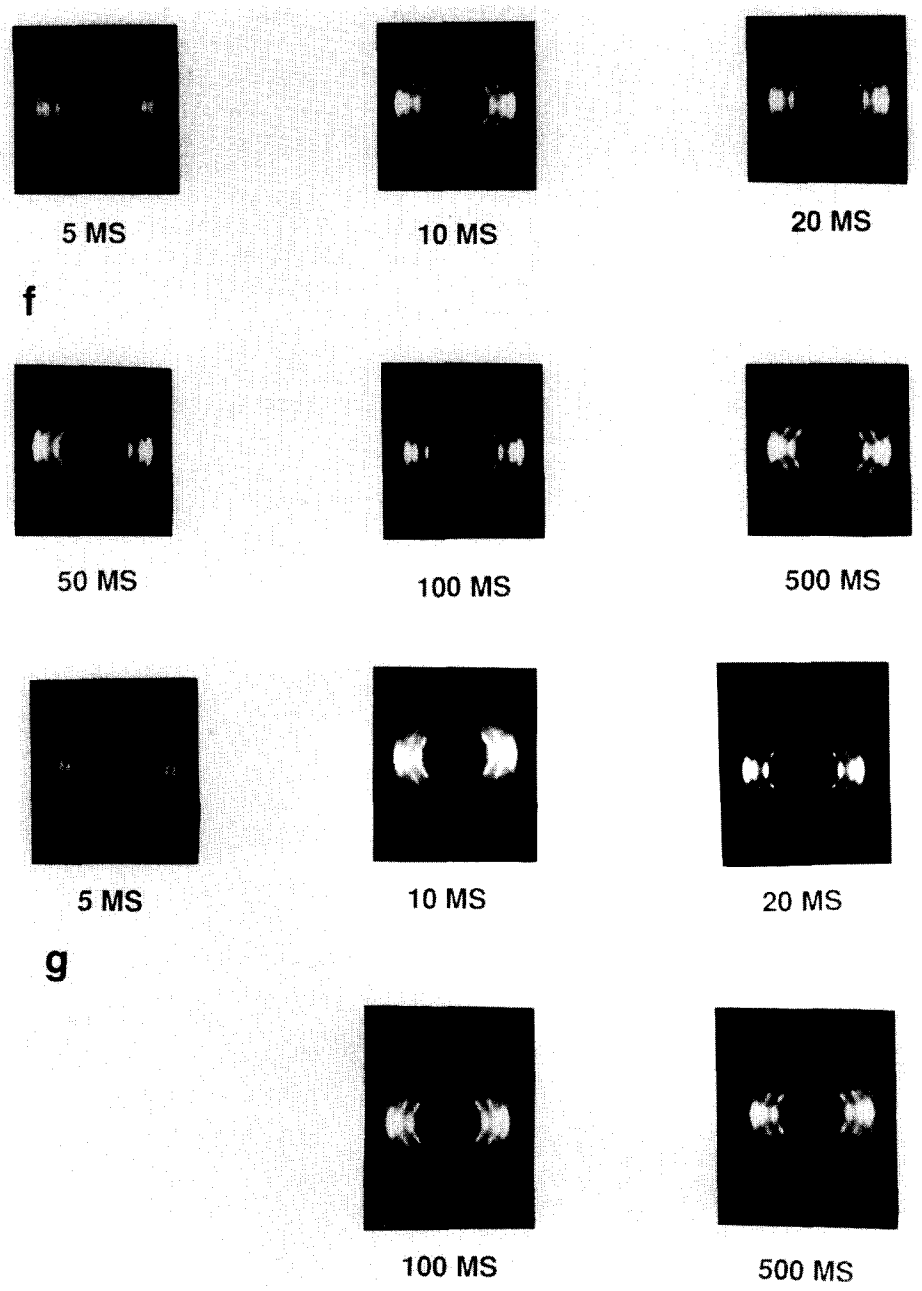

Figure 10 *continued*

temperature and the longer the annealing time, the more clear and better defined are the crystalline reflections. This implies that the crystallites formed at high temperature are more perfect than those formed at low temperature. The crystalline phase emerges at shorter annealing time for higher annealing temperatures.

At 100°C, crystallization does not begin until some time between 50 and 100 ms. The crystalline domains formed at 100 ms are highly defective and/or small, as indicated by the strong overlapping of the crystalline reflections along the equator. Also, their azimuthal angular spread is high (i.e. the orientation of these crystallites is not high). At 500 ms, the crystalline reflections are more discernible (along the radial direction), but their orientations are still low. The observable crystal reflections at 100 ms and 100°C indicate that the crystallization rate at our annealing threadline force increased at least 10-fold above that reported in Peszkin *et al.*[14] (no crystallization at 1000 ms).

At 120°C, crystallization began between 15 and 20 ms, but the crystalline reflections are still vague. At 50 ms, radially discrete reflection peaks show up, but the azimuthal angular spreads are still high (overlapping each other). The crystalline reflections are still not discrete along the azimuth at all annealing times (15 to 930 ms).

At 10 ms and 140°C, the halo begins to concentrate (oriented mesophase) on the equator and there is no indication of the existence of discernible crystalline peaks. Clear crystalline reflections emerge at 20 ms. The orientation of the crystallites increases at longer annealing times, as indicated by the better-defined reflection spots along the azimuth.

The crystalline phase begins to appear at 10, 5 (vague reflections), 5 (clear) and 5 ms (very clear) for 160, 180, 200 and 220°C, respectively. The orientation of crystallites to the fibre axis increases with annealing temperature.

Small-angle X-ray scattering (SAXS)

(a) Isointensity contours. Two-dimensional isointensity SAXS contour maps were produced at several levels of heat-treatment time for fibres annealed at different temperatures. A collection of such maps for thermal treatments at 100 and 160°C are shown in *Figures 11* and *12*. Except for the annealing times at which changes take place, SAXS contour map sets at other temperatures are similar to those seen for 160°C.

At 100°C, the isointensity contours change shape with treatment time, but no obvious interference maximum appears on the meridian. However, the scattering intensity is low for resolution of such a maximum. The corresponding WAXS pattern indicates that the crystalline phase has emerged. This leads us to believe (a) that the crystallites formed at this temperature are defective and the density modulation between amorphous and crystalline phases is low and/or (b) that the number of scattering entities is low.

At 160°C, an obvious change in shape of intensity contours happens at 10 ms. At this time the SAXS intensity begins to increase (see below), indicating that a density modulation begins to set in. In WAXS patterns for this temperature, the crystalline phase also appears at 10 ms.

It is noted that, for all temperatures whenever the crystallite phase emerges in the WAXS patterns, the corresponding SAXS isointensity contours become

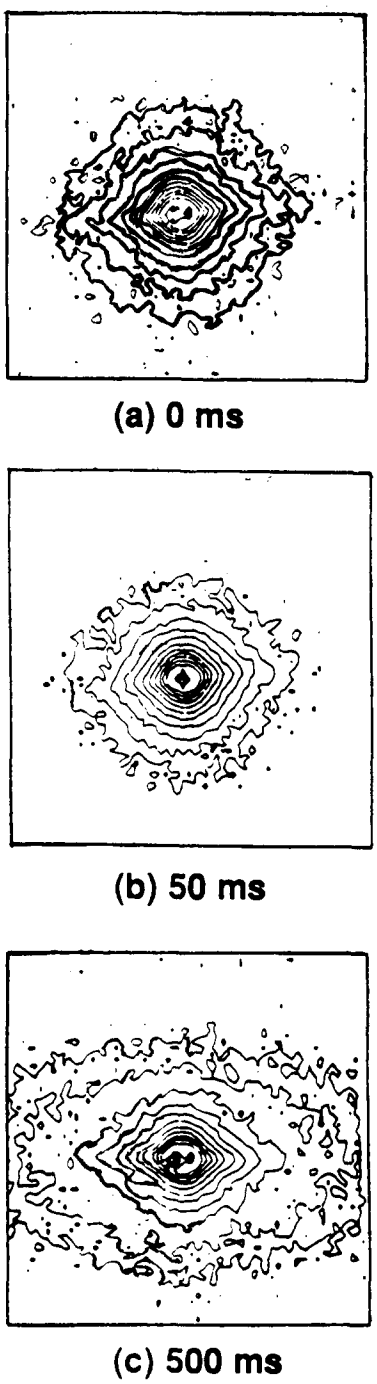

Figure 11 Evolution of SAXS pattern of PET fibres during annealing at 0.083 g/d and 100°C. The fibre axis is in the vertical direction

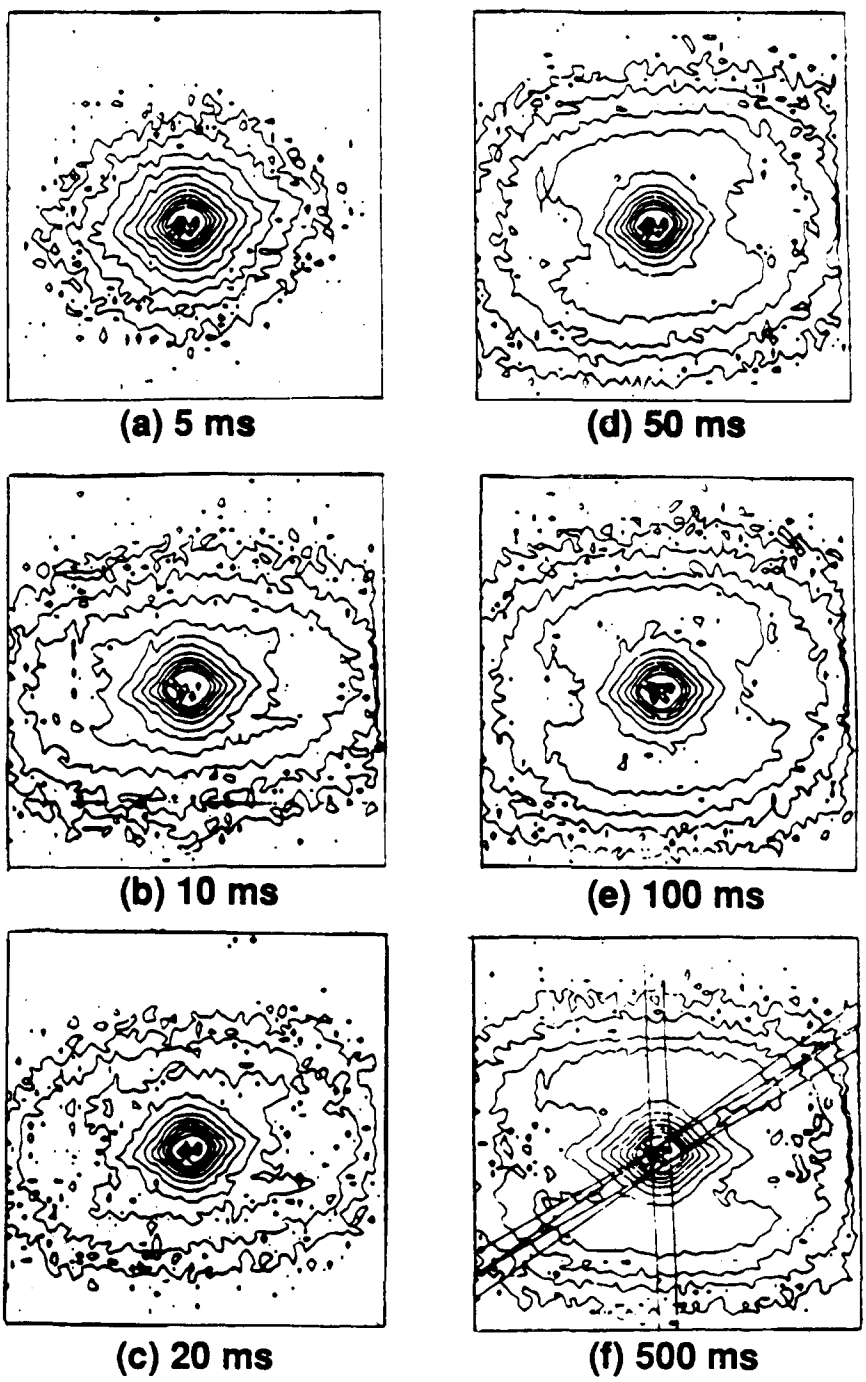

Figure 12 Evolution of SAXS pattern of PET fibres during annealing at 0.083 g/d and 160°C. The fibre axis is in the vertical direction

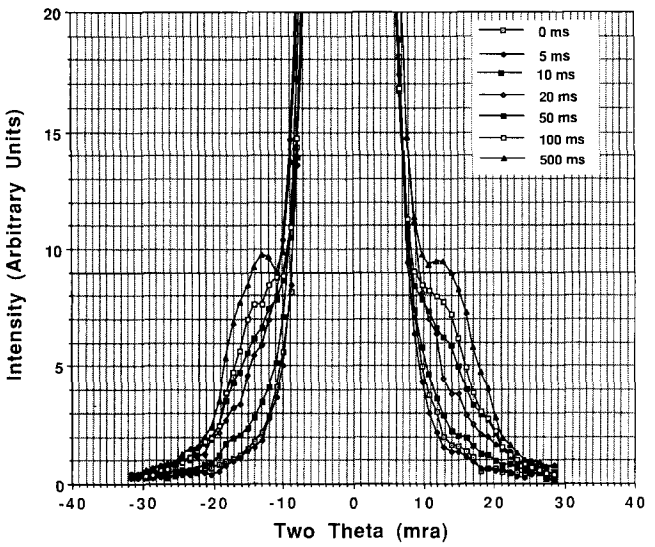

Figure 13 Evolution of SAXS intensity along the fibre axis for PET fibres during annealing at 0.083 g/d and 160°C

elongated perpendicular to the fibre axis, indicating the formation of a fibrillar morphology. That the transverse elongation of intensity is associated with microfibril formation and not elongated voids is demonstrated by the transmission electron microscopy of Chang. He finds no voiding in PET fibres[36] and films[19] exhibiting lateral intensity elongation, but directly observes microfibrillar entities. At higher temperatures, such as 200 and 220°C, the times for change in SAXS patterns as well as WAXS patterns are shorter than 5 ms (our shortest annealing time). The characteristic times (discussed above) for 120, 140, 160 and 180°C are 50, 20, 10 and 5 ms, respectively.

(*b*) *Axial intensity scans.* Additional information can be obtained by scanning the SAXS pattern along the fibre axis and averaging over the width of the scanned channel at each angular position.

Figure 13 is illustrative of such axial scans. This nest of axial intensity curves is for fibres heat treated at 160°C and corresponds to the SAXS contour plots of *Figure 12*. For the axial scan, intensity was tracked along axial bands such as that shown in *Figure 12* at 500 ms. It is noted that the positions of the Bragg maxima are invariant during crystallization (at each temperature above 120°C). The net intensity increase and the long spacing are not evident at low temperatures, such as 100 and 120°C. The long spacings computed from the SAXS maximum positions increase with annealing temperature, as shown in *Figure 14*.

The SAXS Bragg lobes manifest an axial modulation in mass density, typical in polymers of alternating crystalline and non-crystalline regions. It is likely that in the present case the onset and development of SAXS maxima correspond to a fibrillar to lamellar microstructural transition (see below).

The areas under the net intensity increase (over that of the as-spun fibre) curves (often referred to as integrated intensity) are plotted against annealing time in *Figure 15*. Using a simple two-phase approximation, the integrated intensity Q_0 may be written:

$$Q_0 \propto (\rho_c - \rho_a)^2 \phi_c (1 - \phi_c) \qquad (2)$$

where ρ_c and ρ_a are the densities of the crystalline and amorphous phases, respectively, and ϕ_c is the volume fraction of the crystalline phase. An integrated intensity increase is due to an increase in the density modulation and/or the volume fraction of the crystalline phase.

As seen in *Figure 15*, annealing temperature has a marked effect on the integrated SAXS intensity evolution. At a high temperature such as 220°C, the integrated intensity continues to rise pronouncedly between 100 and 500 ms, while, in this time range, most of the other developments have stopped, except for mass density, which shows the same trend but at a slower rate. The higher the temperature, the higher is the evolution rate in integrated SAXS intensity and the higher is the asymptotic integrated intensity.

Mechanical properties. In the cold drawing of PET fibre, there are three stages in the stress–strain curve. The first stage represents an elastic response. As stress increases, a slight drop of the drawing stress is followed by a continuous deformation proceeding at a constant load. This is the stage of plastic deformation. A neck forms at the beginning of this period. In the third stage, strain hardening begins and the orientation of molecules increases with extension. Chains are highly oriented and

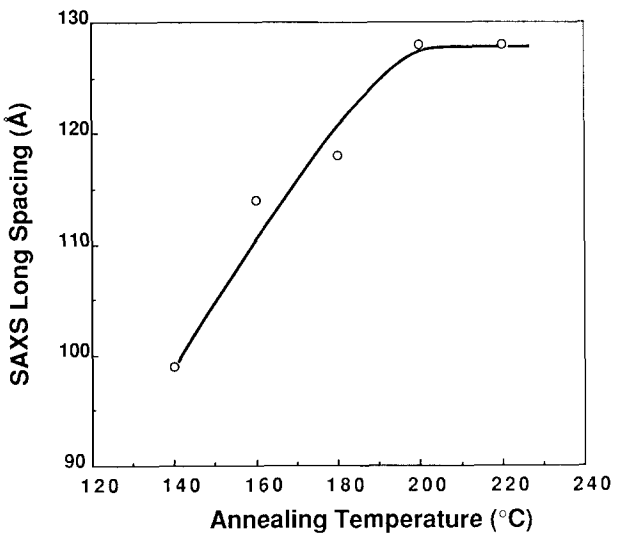

Figure 14 SAXS long spacing *versus* annealing temperature

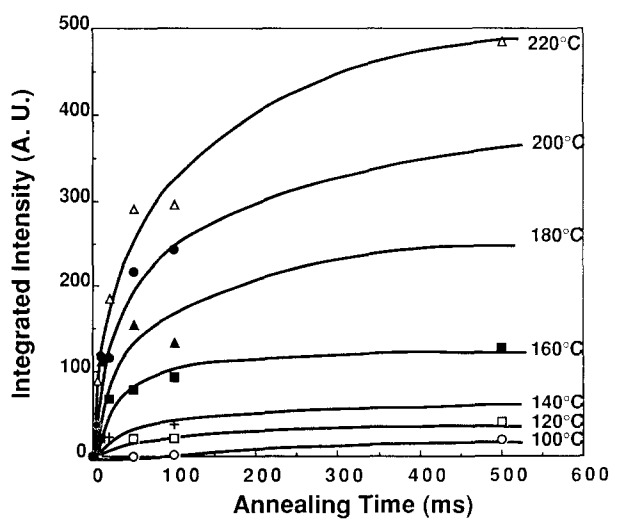

Figure 15 Evolution of the integrated SAXS intensity for PET fibres annealed at 0.083 g/d and different temperatures

likely form oriented mesophase domains that constrain the chains around them. A remarkable increase is noted in the tensile modulus of fibres deformed at room temperature into this stage.

Stress–strain curves of as-spun fibres cold drawn to various extents have been measured. The tensile modulus has been obtained from the initial slope of these curves. These data are shown in *Figure 8*. Also shown here are the 80°C shrinkage data on the same materials. There is little change in the tensile modulus in the first stage of drawing (when the strain is below 60%). In this same range, the 80°C shrinkage increases with deformation. If the shrinkage is linked to the existence in substantial numbers of taut tie molecules and to the absence of constraints to their re-coiling, it would appear that the processes involved in this stage of plastic deformation include increasing the length of such taut molecules and/or loosening the constraints on them. When the deformation is more than 60%, a steady increase in tensile modulus is observed, coupled to a steady decrease in 80°C shrinkage. When the deformation is over 60%, chains are highly oriented, but the ability of chains to re-coil is suppressed.

As mentioned earlier, the appearance of crystallites, if they are aligned to the fibre axis, also contributes to an increase in tensile modulus. *Figure 16* shows the evolution of tensile modulus of fibres annealed at different temperatures. It is noted that the tensile modulus of the annealed fibres increases with annealing time. Furthermore, higher annealing temperature promotes an increase in tensile modulus. The modulus increase is accompanied by an increase in tenacity, as can be seen in *Figure 17*. The tenacity increases with annealing time and annealing temperature.

Both the asymptotic tensile modulus and tenacity have linear relationships with the annealing temperature, as depicted in *Figures 18* and *19*. The higher the annealing temperature, the higher the asymptotic tensile modulus and tenacity.

Correlations

The discussion centres here on kinetic correlations among the characteristics measured. Such comparisons provide evidence towards the processes involved and towards what features are important in determining the kinetics and final mechanical properties.

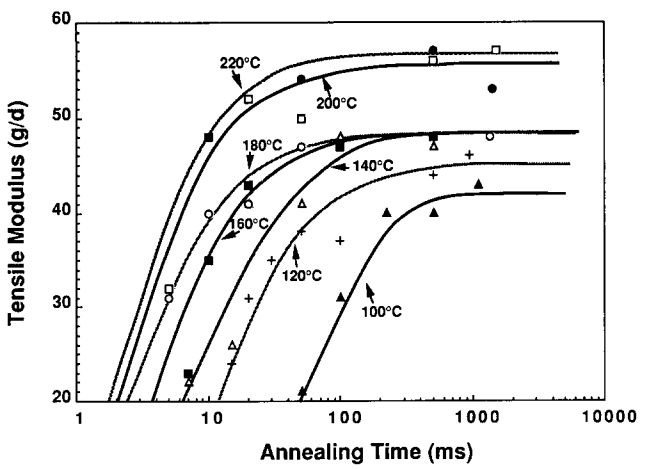

Figure 16 Evolution of the tensile modulus of PET fibres annealed at 0.083 g/d and different temperatures

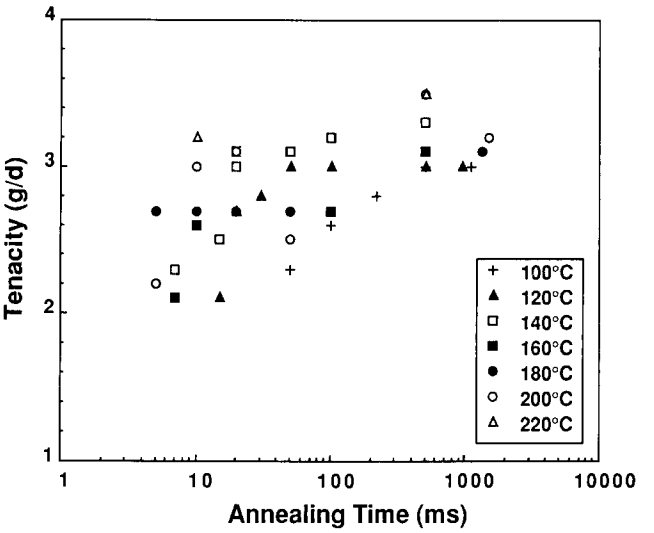

Figure 17 Evolution of the tenacity of PET fibres annealed at 0.083 g/d and different temperatures

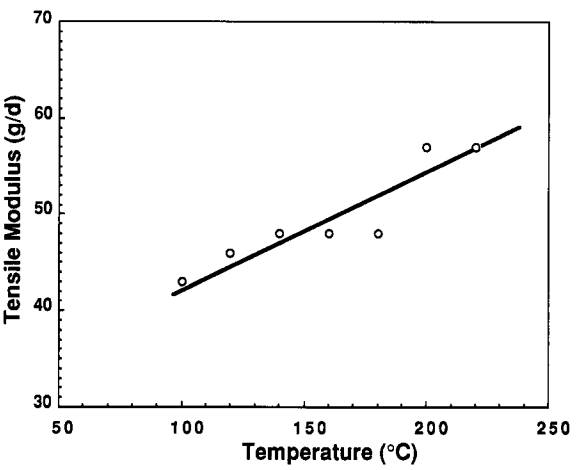

Figure 18 Asymptotic tensile modulus of PET fibres annealed at 0.083 g/d and different temperatures

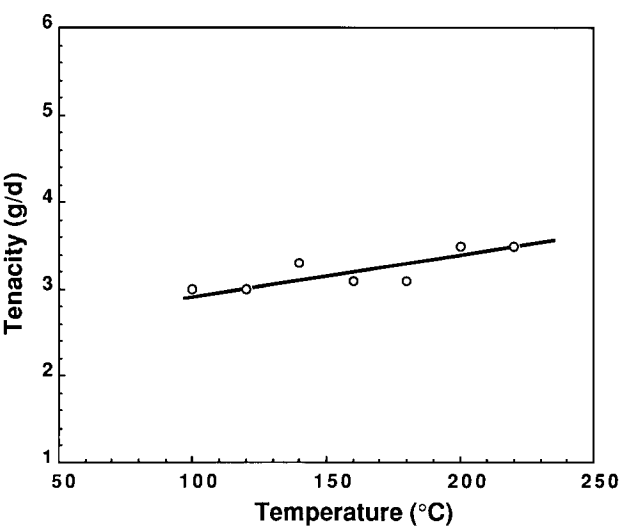

Figure 19 Asymptotic tenacity of PET fibres annealed at 0.083 g/d and different temperatures

The incubation periods for the start of elongation and shrinkage at 80°C, the emergence in WAXS of crystalline peaks and the increases in density and tensile modulus are coincident. Comparing the density, the elongation,

the shrinkage at 80°C and the integrated SAXS intensity evolution curves, however, one can see that the elongation and the shrinkage at 80°C approach their asymptotic value earlier than do the density and the integrated SAXS intensity. This seems to suggest that there are two stages of crystallization. In the first stage, the fibres elongate and the shrinkage is suppressed by the structure developed in this period. In the second stage, as the crystals become more perfect, mass density and integrated SAXS intensity (density modulation) continue to rise with annealing time. Evidence towards these suggestions is further provided in the following.

Elongation versus *density.* Two different behaviours are noted in the relationship between the elongation and the density, as shown in *Figure 20.* When the elongation is below 35%, the density increases very slowly with elongation. It is not unreasonable to attribute this behaviour to the formation of a highly defective crystalline phase or to a mesophase that produces only a slight increase in the mass density. In the later stage of crystallization, when the elongation is over 35%, the density increases abruptly while the elongation approaches its asymptotic value. This may be attributed to the rearrangement of chains in crystals to reach more stable positions and to the consequent increase in perfection and mass density of the crystallites.

Elongation versus *shrinkage at 80°C.* The elongation and the shrinkage at 80°C appear to follow a linear relationship, as shown in *Figure 21.* This leads to the suggestion that some structural feature developed in the elongation process has a dominant effect on the shrinkage. This structural feature is likely a highly defective crystalline phase, as indicated by the corresponding WAXS patterns. These crystallites anchor the chains in the amorphous area around them. The mobility of these chains is, therefore, reduced.

Density versus *shrinkage at 80°C. Figure 22* shows the density *versus* shrinkage at 80°C for all annealing conditions. There are two trends in this figure. At the lower right portion (when the shrinkage is over 20%), the density increases only slightly with an abrupt decrease in the shrinkage at 80°C. This observation suggests that this period is the early stage of crystallization, in which highly defective and small crystallites form,

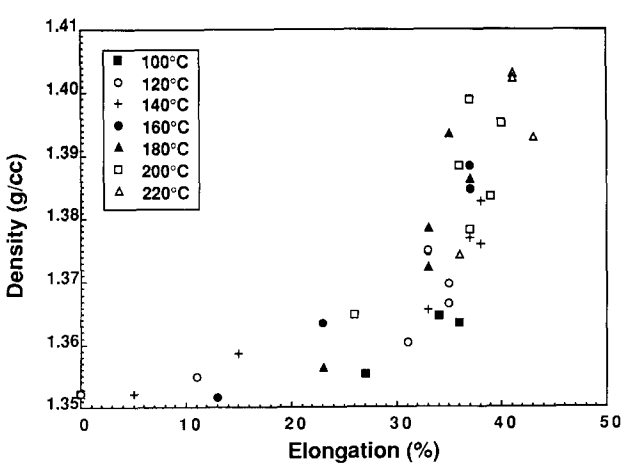

Figure 20 Plot of elongation *versus* density for annealed PET fibres

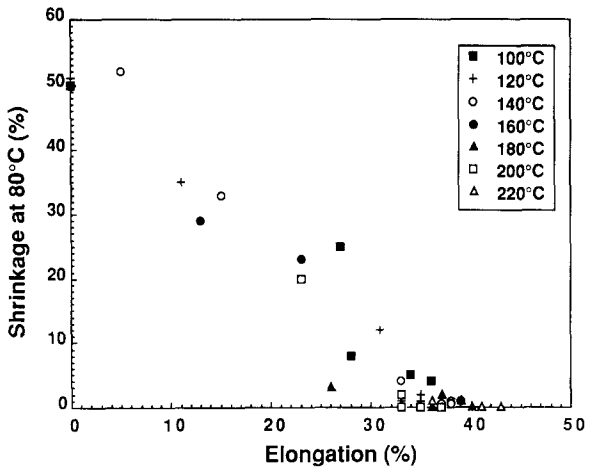

Figure 21 Plot of elongation *versus* shrinkage at 80°C for annealed PET fibres

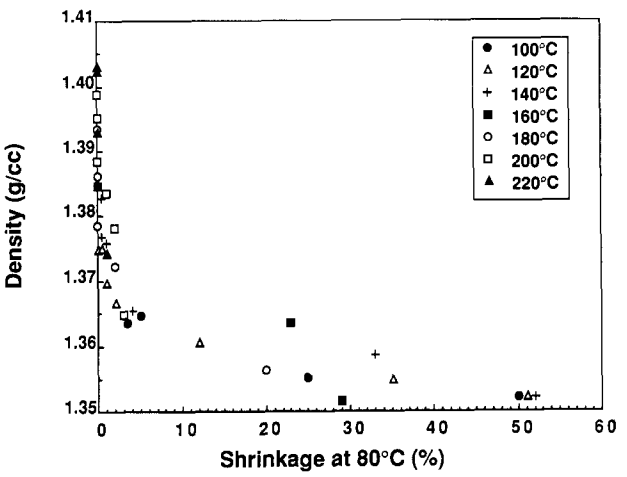

Figure 22 Plot of density *versus* shrinkage at 80°C for annealed PET fibres

producing little increase in the density, but with tremendous effect on suppression of chain re-coiling. When the shrinkage falls below 10%, the density increases abruptly. As 0% shrinkage is approached, the density rises nearly vertically. This evidences a second stage of crystallization during which crystals become more perfect.

Density versus *tensile modulus.* As shown in *Figure 23,* the tensile modulus increases with the mass density of the annealed fibres. The rate of increase of modulus with density is relatively rapid up to a density of approximately 1.37 g cm^{-3}. Beyond this level, the modulus increases more slowly. In *Figure 20,* it is this density, 1.37 g cm^{-3}, that marks the end of the processing regime in which fibrillar crystals were created. Thus the initial, more rapid increase in stiffness develops with fibrillar crystals, while the somewhat slower increase relates to further rearrangement of the chains. This latter stage likely includes a fibrillar to lamellar transition, as observed by Chang in PET films[19,36] and fibres[36]. A sketch of the stages of fibrillar to lamellar transition, based on Chang's observations and on earlier observations in polypropylene[37], is given as *Figure 24.* The disappearance of the fibrillar connection is believed to be required for the propagation of a front, which would laterally

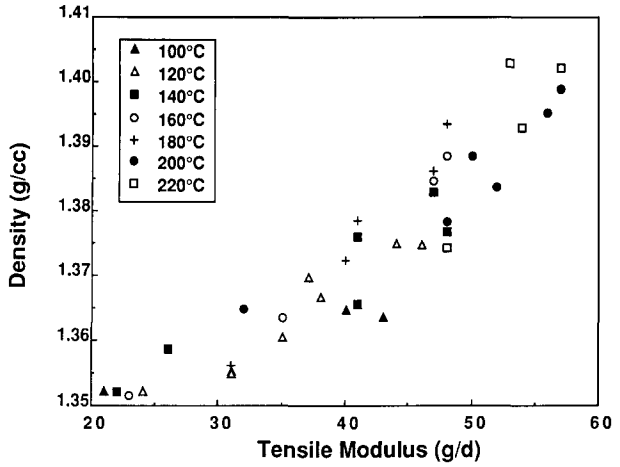

Figure 23 Plot of density *versus* tensile modulus for annealed PET fibres

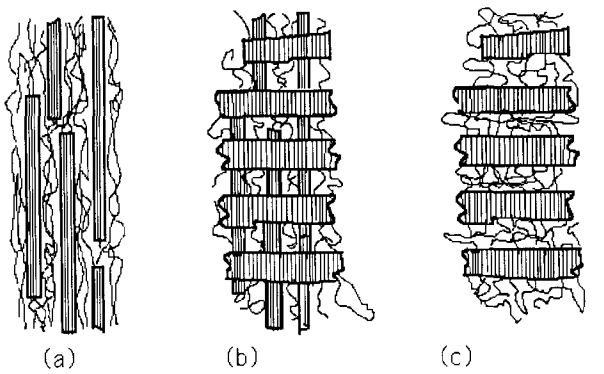

Figure 24 Stages in the fibrillar to lamellar transition: (a) initial state, microfibrillar crystals; (b) lateral growth of crystals; (c) disappearance of traces of initial microfibrils

weld together crystallites with different initial orientations[37]. In the lamellar microstructure, crystalline and amorphous phases are in series and the modulus would necessarily be lower than for the case of an equivalent mass fraction of fibrillar crystallites in parallel with the non-crystalline material. In the present work, the increasingly serial microstructure is evidenced by a strong increase in the intensity of the axial SAXS Bragg peak during the second stage of crystallinity development.

Tensile modulus versus *elongation.* *Figure 25* shows the elongation *versus* tensile modulus for all annealing conditions. Two relationships are noted in this figure. When the elongation is below 35%, the tensile modulus increases with increasing elongation and the relationship seems to be linear. This relationship breaks down at approximately 35% elongation; here, elongation reaches its asymptotic value, while the tensile modulus continues to increase. The modulus increase in this region is via increasing degree of crystallinity and increasing perfection of the crystallites. The modulus increase below an elongation of 35% would again appear to be associated with the development of a microfibrillar system.

Shrinkage at 80°C versus *tensile modulus.* The relationship between the tensile modulus and the shrinkage at 80°C can be divided into two regions, as shown in *Figure 26.* In the upper left corner, the correlation seems to be linear. However, in the lower right portion, the modulus still increases, while the shrinkage falls to zero. In the early stage of crystallization, many defective crystals form and their presence restricts the mobility of the chains in the amorphous regions, thereby both increasing the tensile modulus and decreasing the ability to shrink. When the crystals formed in the first stage have refined themselves into a serial crystal/amorphous array, the non-crystalline chains relax, thereby obviating the driving force for axial shrinking.

Density versus *tenacity.* *Figure 27* shows that tenacity increases with increasing mass density, implying that the extent of crystallization contributes to the tenacity increase.

Crystallization kinetics

Figure 28 shows the transformation half-time of the evolution of density *versus* annealing temperature. Plotted are data both from the present work and from Peszkin *et al.*[14]. The crystallization rate is enhanced remarkably by the threadline tension.

Processing–structure–property relationship

The threadline stress used here surpasses the re-coiling force of the molecules in the fibre and orients these

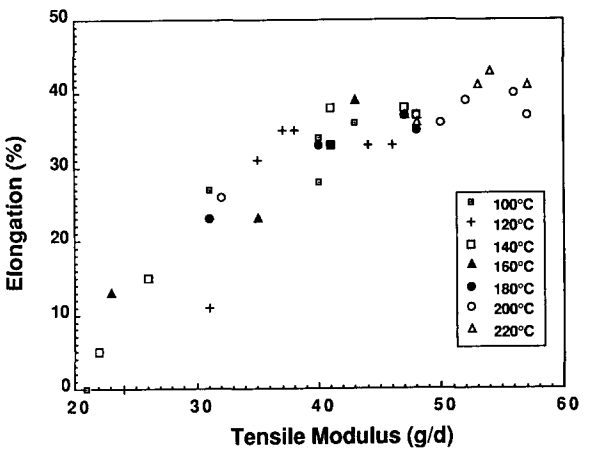

Figure 25 Plot of elongation *versus* tensile modulus for annealed PET fibres

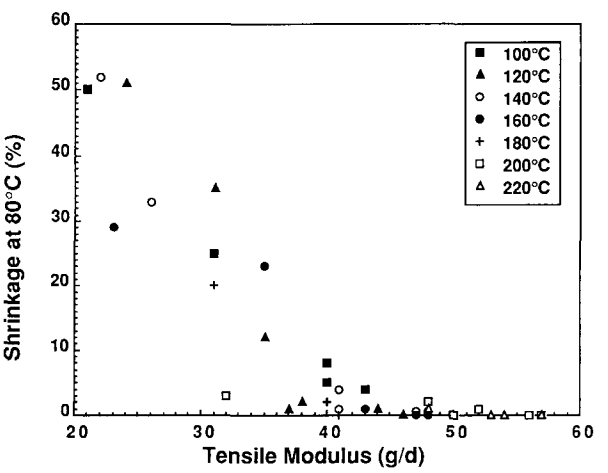

Figure 26 Plot of tensile modulus *versus* shrinkage at 80°C for annealed PET fibres

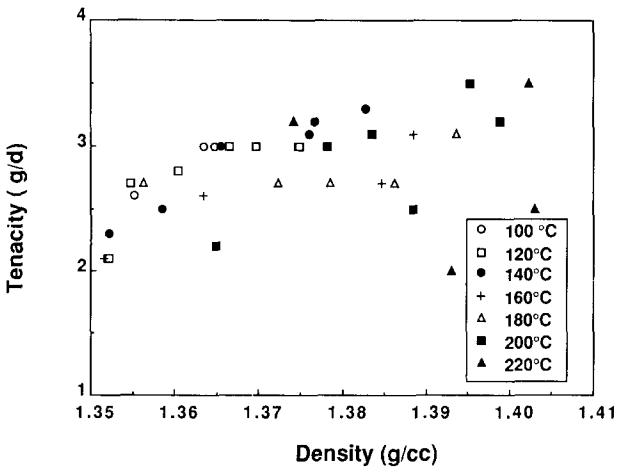

Figure 27 Plot of density *versus* tenacity for annealed PET fibres

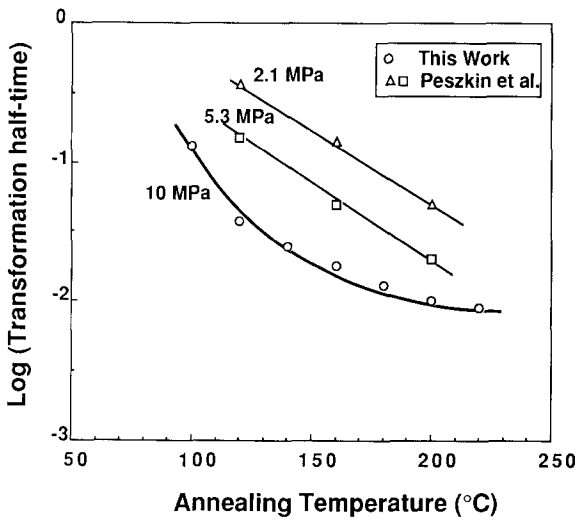

Figure 28 Transformation half-time *versus* temperature. The stress is indicated beside the curves. The data of Peszkin *et al.* are from ref. 14

molecules to the fibre axis and thus enhances the crystallization rate during annealing. Moreover, this stress restricts non-crystalline chains between crystalline and amorphous regions from disorienting with respect to the fibre axis. The crystallites formed under these conditions and the high orientation of the taut tie chains to the fibre axis contribute to the increase in the tensile modulus of the annealed fibres. The major modulus increase happens in the first stage of crystallization, while the modulus increases more slowly and attains its asymptotic value during a second stage. The dimensional stability of the fibres is set in the first stage of crystallization, when the fibres elongate and crystallization begins. The tenacity follows the trend of the tensile modulus.

The results obtained here are of potential utility in fibre manufacture. For PET fibres annealed under threadline tension (10 MPa), the tensile modulus increases with annealing temperature and annealing time (before the asymptotic value for each temperature is reached). The higher the annealing temperature, the shorter is the characteristic time for reaching the asymptotic value. If tensile modulus is the primary concern for optimizing this process, then the condition for achieving the highest modulus increase is to anneal the fibres at 220°C for 50 ms for the tension used in this work. If, on the other hand, economy of operation is most important, annealing should be done at a more moderate temperature, such as 140°C, and a higher tension (> 10 MPa), for 100 ms. Higher threadline tension will promote a greater increase in modulus, which can compensate the modulus difference between 140 and 220°C, if the annealing is done at the same tension level. Furthermore, the enhanced crystallization rate under high threadline tension may shorten the annealing time needed for the modulus to reach its asymptotic value.

SUMMARY

Fibres were annealed under a stress of 0.083 g/d (1×10^8 dyn cm^{-2}) for a series of time intervals, ranging from 5 ms to 1.2 s, and at different temperatures, ranging from 100 to 220°C.

Dual behaviours are found in the relationships between the density and the elongation; the density and the shrinkage at 80°C; the elongation and tensile modulus; and the shrinkage at 80°C and tensile modulus. Therefore the crystallization during annealing is envisioned as occurring in two stages. In the first stage, nucleation begins and fibrillar crystallites grow as the fibres begin to elongate. Chain mobility in the non-crystalline material is restricted gradually and reaches its asymptotic value in this period. Concurrently, tensile modulus and tenacity increase markedly in this period. In the second stage, a lamellar microstructure is created and the perfection of crystallites continues to increase. In this second stage, fibre elongation during heat treatment reaches its asymptotic value. Simultaneously, the increasing trend in tensile modulus slows down and reaches its asymptotic value.

ACKNOWLEDGEMENTS

The support of Rhone-Poulenc and E. I. du Pont de Nemours is gratefully acknowledged. The continuous support, interest and contributions of Dr Randolph Barton Jr of Du Pont and the generous access, through him, to Du Pont facilities are greatly appreciated. Dr John Hearle of UMIST has followed this work closely and has advised us at all stages. For this we are grateful.

REFERENCES

1 Cobbs, W. H. and Burton, R. L. *J. Polym. Sci.* 1953, **10**, 275
2 Statton, W. O. *Am. Chem. Soc., Div. Polym. Chem., Prepr.* 1966, **7**, 31
3 Baranov, V. G., Kenarov, A. V. and Volkov, T. I. *J. Polym. Sci. (C)* 1970, **30**, 271
4 van Antwerpen, F. and van Krevelen, D. W. *J. Polym. Sci., Polym. Phys. Edn* 1972, **11**, 2423
5 Dumbleton, J. H. *J. Polym. Sci. (A-2)*, 1969, **7**, 667
6 Matyi, R. J. and Crist B. Jr *J. Macromol. Sci.–Phys. (B)* 1979, **16** (1), 15
7 Smith, F. and Steward, R. D. *Polymer* 1974, **15**, 283
8 Alfonso, G. C., Verdona, M. P. and Wasiak, A. *Polymer* 1978, **19**, 711
9 Althen, G. and Zachmann, H. G. *Makromol. Chem.* 1979, **180**, 2723
10 Fischer, E. W. and Fakirov, S. *J. Mater. Sci.* 1976, **11**, 1041
11 Fakirov, S., Fischer, E. W., Hoffmann, R. and Schmidt, G. F. *Polymer* 1977, **18**, 1121
12 Gupte, K. M., Motz, H. and Schultz, J. M. *J. Polym. Sci., Polym. Phys. Edn* 1983, **21**, 1927
13 Itoyama, K. *J. Polym. Sci., Polym. Phys. Edn* 1987, **25**, 331

14 Peszkin, P. N., Schultz, J. M. and Lin, J. S. *J. Polym. Sci., Polym. Phys. Edn* 1986, **24**, 2591
15 Tiller, W. A. and Schultz, J. M. *J. Polym. Sci., Polym. Phys. Edn* 1984, **22**, 143
16 Ziabicki, A. and Jarecki, L. 'High-Speed Fiber Spinning' (Eds A. Ziabicki and H. Kawai), Wiley, New York, 1985, Ch. 9
17 Schultz, J. M. *Polymer* 1991, **31**, 661
18 Hristov, H. A. and Schultz, J. M. *J. Polym. Sci., Polym. Phys. Edn* 1990, **28**, 1647
19 Chang, H., Schultz, J. M. and Gohil, R. M. *J. Macromol. Sci.–Phys.* 1993, **B32**, 99
20 George, H. H., Hole, A. and Buckley, A. *Polym. Eng. Sci.* 1983, **23**, 95
21 Cheng, J., Guan, X., Wei, R. and Ma, H. *Int. Polym. Process.* 1988, **3**, 95
22 Ikeda, R. M. *J. Polym. Sci., Polym. Lett. Edn* 1980, **18**, 325
23 Adams, G. C. *Polym. Eng. Sci.* 1979, **19**, 456
24 Wilson, M. P. W. *Polymer* 1974, **15**, 277
25 Dismore, P. F. and Statton, W. O. *J. Polym. Sci. (C)* 1966, **13**, 133
26 Statton, W. O., Koenig, J. L. and Hannon, M. *J. Appl. Phys.* 1970, **41**, 4290
27 Dumbleton, J. H. *Polymer* 1969, **10**, 539
28 Dumbleton, J. H. *J. Polym. Sci. (A-2)* 1969, **7**, 667
29 Hendricks, R. W. *J. Appl. Crystallogr.* 1978, **11**, 5
30 American Society for Testing of Materials, 'Method of Test for Densities of Plastics by the Density Gradient Technique', D1505-63T, 1964
31 American Society for Testing of Materials, D1776, 1985
32 Lindner, W. L. *Polymer* 1973, **14**, 9
33 Jellinke, G., Ringens, W. and Heidemann, G. *Ber. Bunsenges. Phys. Chem.* 1970, **74**, 924
34 Gupta, V. B. and Kumar, S. *Polymer* 1978, **19**, 953
35 Peterlin, A. 'Ultra High Modulus Polymers' (Eds A. Ciferri and I. M. Ward), Applied Science, London, 1979
36 Chang, H., Ph.D. Dissertation, University of Delaware, 1991; Chang, H. and Schultz, J. M. *J. Macromol. Sci.-Phys.* in press
37 Schultz, J. M. and Petermann, J. *Colloid Polym. Sci.* 1984, **262**, 294